SLAC NATIONAL ACCELERATOR LABORATORY

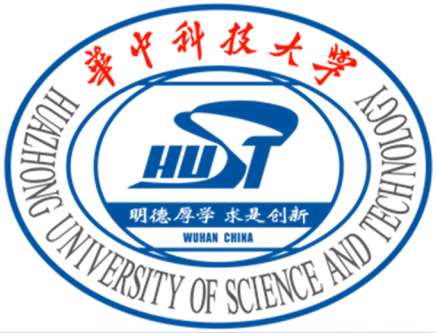

39th International Free-Electron Laser Conference

FEL19

Hamburg, Germany

26-30 August 2019

Universität Hamburg, Main building

Physics of post-saturation tapered FEL towards single-frequency terawatt output power

Cheng-Ying Tsai

State Key Laboratory of Advanced Electromagnetic Engineering and Technology

Huazhong University of Science and Technology (HUST)

Outline

- ❑ Motivations to terawatt (TW) x-ray FEL
- ❑ Theoretical approaches to TW XFEL
  - ● the scope of this presentation
- ➢ **Part I**: Sideband instability
- Summary and discussion
- ➢ **Part II**: Radiation diffraction in the post-saturation regime
- Summary and discussion
- ➢ **Part III**: Area-preserving undulator tapering
- Summary and discussion
- ❑ Acknowledgements

Scientific motivations

➢ Coherent diffraction imaging

- Femtosecond laser pulse, “diffraction-before-destruction” technique
- Coherent diffractive imaging of biological samples with XFEL

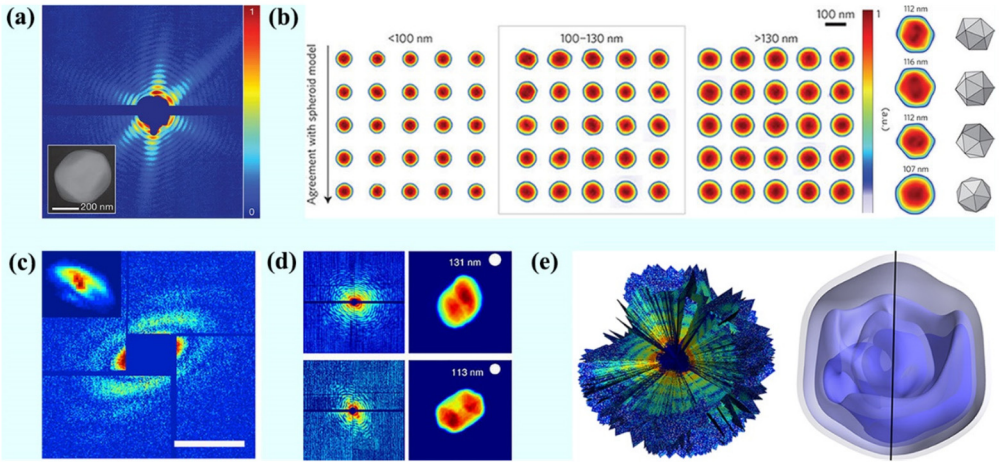

Sun *et al.*, Current Status of Single Particle Imaging with X-ray Lasers, Appl. Sci. 2018, 8(1), 132

➢ High field electrodynamics

- Femtosecond laser pulse, extremely high power density
- Nonlinear x-ray processes in crystals, test/search strong-field QED phenomena, etc

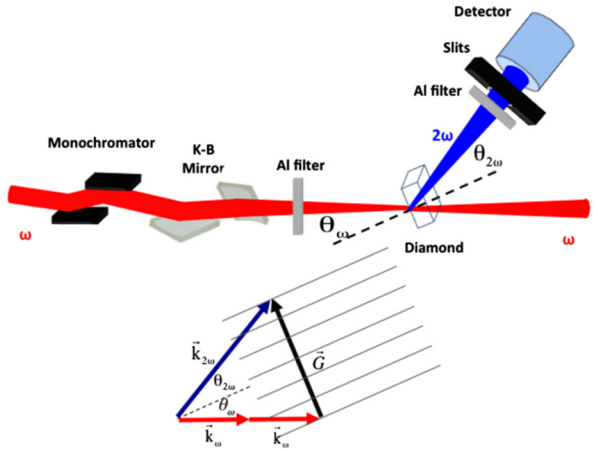

Shwartz *et al.*, X-Ray Second Harmonic Generation, PRL 112, 163901 (2014)

➢ Single-molecule imaging

- Femtosecond laser pulse, high-repetition rate operation
- Single-molecule scattering and photon correlations

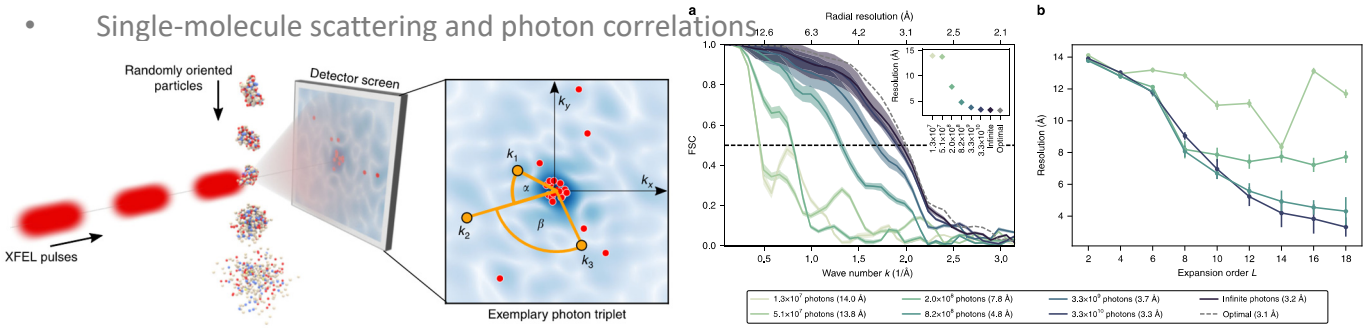

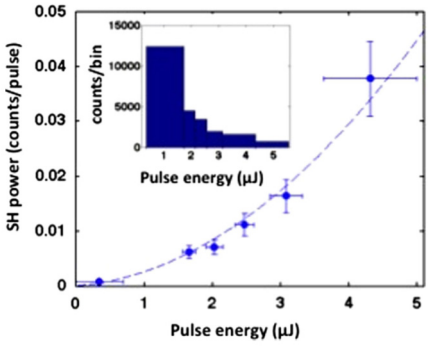

von Ardenne *et al.*, Structure determination from single molecule X-ray scattering with three photons per image, Nature Comm., vol. 9, 2375 (2018)

Motivation

- The above applications set requirements for the laser beam with
  - femtosecond pulse duration
  - number of photons 10^{12}-10^{14}/pulse
  - photon energy 5~10 keV, pulse energy 5~10 mJ (fundamental mode)

➢ All these correspond to XFEL output power of 1 TW or higher in a (tens of) femtosecond pulse duration

- Order of magnitude estimate for typical XFEL parameters, the output performance at initial saturation

$$I_{\mathrm{b}}^{\mathrm{pk}} \sim \mathrm{kA},\ E_{\mathrm{b}} \sim \mathrm{GeV},\ \sigma_{\perp} \sim 20\ \mu\mathrm{m},\ L_U^{\mathrm{tot}} \sim 50\ \mathrm{m},\ \lambda_u \sim \mathrm{cm},$$

$$\rho \sim 10^{-3} \Rightarrow P_{\mathrm{rad}} \approx \rho P_{\mathrm{beam}} \sim 25\ \mathrm{GW}$$

Still a factor of 20~40 before reaching the goal of TW power level

Theoretical studies for TW XFEL

Methodology

- **Analytical/Semi-analytical approach**: simple, idealized model, can give quick estimate, scaling relation
- Numerical simulation: more realistic model, gain physics intuition, suitable for design optimization [e.g., Jiao *et al*. (2012)]

Schemes

- Typical/proposed schemes to achieve TW FEL (to name a few)
  - **undulator tapering**, to retain resonance condition [KMR (1981)] $\lambda_R = \frac{\lambda_u}{2\gamma_R^2}\left(1+\frac{K_0^2}{2}\right)$
  - slotted foil plus laser-electron beam delay between undulator sections [e.g., Tanaka (2013)]
  - add multiple slot foils or transverse tilts, use delays to divide electron beam into different parts [Prat *et al*. (2015)]
  - apply multiple phase shifters to amplify a single/target current spike [Kumar *et al*. (2016)]

Our focus

- In this presentation, we use **semi-analytical approach** and focus on physics involving **undulator tapering** in seeded (x-ray) FEL after saturation, including **sideband instability**, **transverse diffraction**, and **taper scheme** for efficiency enhancement

Part I

FEL SIDEBAND INSTABILITY

Ref: C.-Y. Tsai *et al*., PRAB **20**, 120702 (2017)

FEL simulation (*GENESIS*)

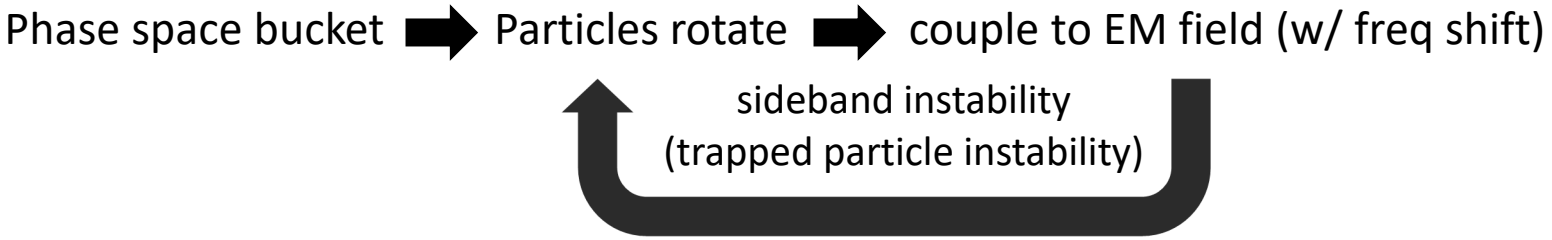

1-D FEL system

- Start from 1-D FEL Hamiltonian (in the absence of sideband)

$$\mathcal{H}(\theta,\eta;\hat{z}) = \frac{(\eta-\eta_R)^2}{2f_R} - i\frac{f_B}{f_R}(\mathcal{E}e^{i\theta} - \mathcal{E}^* e^{-i\theta})$$

- The (2*N*+1) equations of motion

$$\frac{d\theta}{d\hat{z}} = \frac{\partial\mathcal{H}}{\partial\eta} = \frac{\eta-\eta_R}{f_R}$$

$$\frac{d\eta}{d\hat{z}} = -\frac{\partial\mathcal{H}}{\partial\theta} = -\frac{f_B}{f_R}(\mathcal{E}e^{i\theta} + \mathcal{E}^* e^{-i\theta})$$

$$\frac{d\mathcal{E}}{d\hat{z}} = \left(\frac{\partial}{\partial\hat{z}} + \frac{\partial}{\partial\hat{u}}\right)\mathcal{E} = \frac{f_B}{f_R}\langle e^{-i\theta}\rangle$$

- In linear (or exponential) regime, such a system can be well described by the density modulation $b \equiv \langle e^{-i\theta}\rangle$ and the energy modulation $p \equiv \langle \eta e^{-i\theta}\rangle$ (Bonifacio *et al*. 1984)

$$\theta = (k_R + k_u)z - \omega_R t$$

$$\eta = \frac{\gamma-\gamma_{R0}}{\rho\gamma_{R0}}, \eta_R = \frac{\gamma_R-\gamma_{R0}}{\rho\gamma_{R0}}$$

$$\rho = \frac{1}{\gamma_R(0)}\left(\frac{\omega_{pb}K_0/\sqrt{2}}{4ck_u}\right)^{2/3}$$

$$\mathcal{E} = \frac{E}{\sqrt{4\pi n_0\rho\gamma_{R0}m_0c^2}}$$

$$\hat{z} = 2k_u\rho z$$

$$\lambda_R = \frac{\lambda_u}{2\gamma_R^2(0)}\left(1+\frac{K_0^2}{2}\right)$$

$K(\hat{z}) = K_0 f_B(\hat{z})$ taper profile

$\gamma_R(\hat{z}) = \gamma_{R0} f_R(\hat{z})$

$$f_R(\hat{z}) = \sqrt{\frac{1+\frac{1}{2}K_0^2 f_B^2(\hat{z})}{1+\frac{1}{2}K_0^2}}$$

1-D FEL system

- Start from 1-D FEL Hamiltonian (in the absence of sideband)

$$\mathcal{H}(\theta,\eta;\hat{z}) = \frac{(\eta-\eta_R)^2}{2f_R} - i\frac{f_B}{f_R}\left(\mathcal{E}e^{i\theta} - \mathcal{E}^* e^{-i\theta}\right) = \frac{(\delta\eta)^2}{2f_R} + 2\frac{f_B(\hat{z})}{f_R(\hat{z})}|\mathcal{E}|\left[\sin\Theta_R + \sin\Theta - (\Theta+\Theta_R)\cos\Theta_R\right]$$

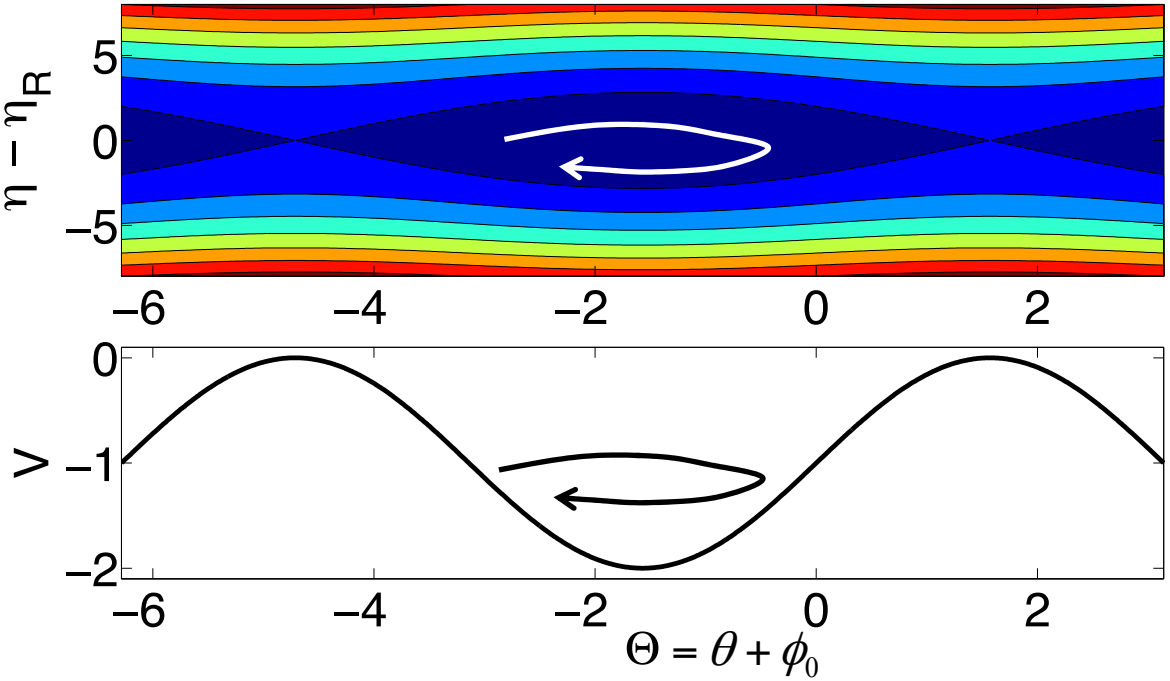

1-D FEL system

- Start from 1-D FEL Hamiltonian (in the absence of sideband)

$$\mathcal{H}(\theta,\eta;\hat{z}) = \frac{(\eta-\eta_R)^2}{2f_R} - i\frac{f_B}{f_R}\left(\mathcal{E}e^{i\theta} - \mathcal{E}^* e^{-i\theta}\right) = \frac{(\delta\eta)^2}{2f_R} + 2\frac{f_B(\hat{z})}{f_R(\hat{z})}|\mathcal{E}|\left[\sin\Theta_R + \sin\Theta - (\Theta+\Theta_R)\cos\Theta_R\right]$$

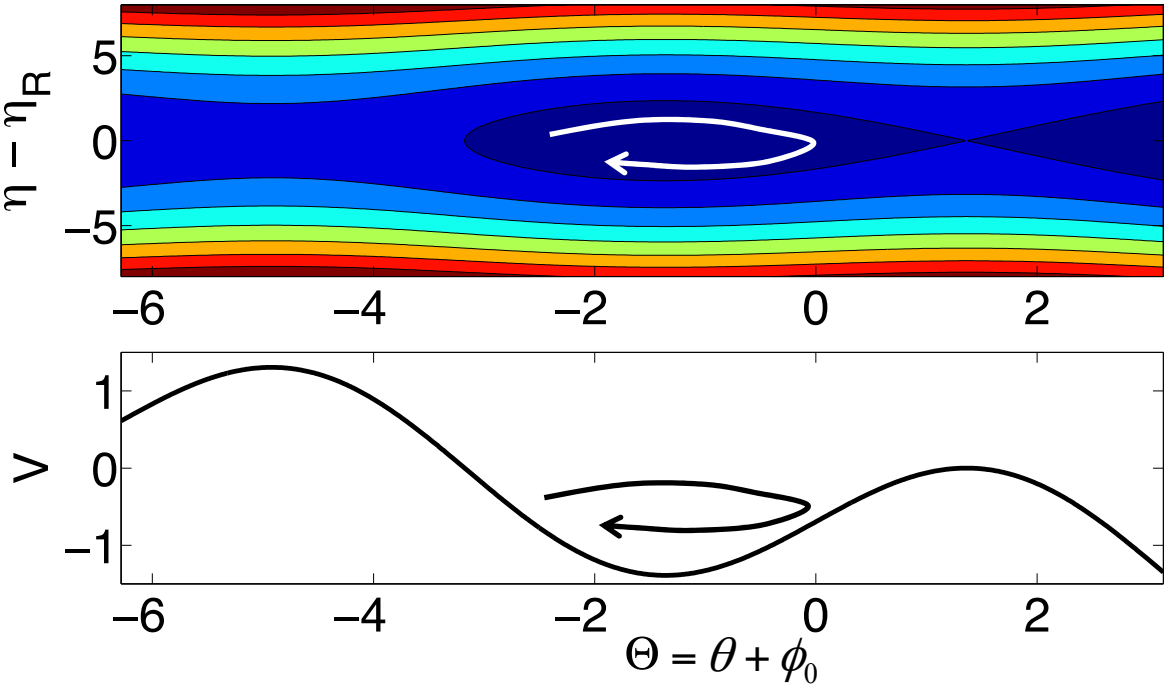

$\Theta_R = -78°$ (tapered)

Macroparticle model

- To proceed with macroparticle approach, we assume that electrons are deeply trapped in the bottom of the potential well
- In the post-saturation regime, in addition to microbunching, the electron beam begins to rotate in the longitudinal phase space with the small-amplitude synchrotron frequency

$$\frac{d^2}{d\hat{z}^2}\delta\theta + \Omega_{\mathrm{syn},0}^2\delta\theta = 0 \qquad \Omega_{\mathrm{syn},0}^2 = -2\frac{f_B}{f_R^2}|\mathcal{E}|\sin\Theta_R$$

- It turns out that such electron synchrotron motion will couple EM wave with frequency shift $\omega_s \approx 2c\gamma_R^2\Omega_{\mathrm{syn},0}$ apart from the main signal
- Usually **undesired**: degrade spectral purity, cause particle detrapping, prevent further growth of the main signal...etc
  - in the following analysis we restrict to onset of the sideband instability

Linear stability analysis

- First order perturbation
  - refer the unperturbed solution to that at first saturation

$$\mathcal{E} = (|\mathcal{E}_0| + \delta\mathcal{E}' + i\delta\mathcal{E}'')e^{i\phi_0}$$

$$\eta = \eta_R + \delta\eta$$

$$\theta = \theta_R + \delta\theta,$$

$$\Theta = \theta + \phi_0,\ \Theta_R = \theta_R + \phi_0 \in \left[\frac{-\pi}{2}, 0\right]$$

$$(\delta\theta, \delta\eta, \delta\mathcal{E}', \delta\mathcal{E}'') \propto \mathrm{Re}(e^{ik\hat{z} - i\kappa\hat{u}})$$

- Stability is determined by the determinant of the matrix

$$\begin{pmatrix} ik & -f_R^{-1} & 0 & 0 \\ f_R\Omega_{\mathrm{syn},0}^2 & ik & 2\frac{f_B}{f_R}\cos\Theta_R & \frac{f_R}{|\mathcal{E}_0|}\Omega_{\mathrm{syn},0}^2 \\ -\frac{f_R}{2|\mathcal{E}_0|}\Omega_{\mathrm{syn},0}^2 & 0 & i(k-\kappa) & -\frac{f_R}{2|\mathcal{E}_0|^2}\Omega_{\mathrm{syn},0}^2 \\ \frac{f_B}{f_R}\cos\Theta_R & 0 & \frac{f_R}{2|\mathcal{E}_0|^2}\Omega_{\mathrm{syn},0}^2 & i(k-\kappa) \end{pmatrix} \begin{bmatrix} \langle\delta\theta\rangle \\ \langle\delta\eta\rangle \\ \delta\mathcal{E}' \\ \delta\mathcal{E}'' \end{bmatrix} = \mathbf{0}$$

- Given κ, solve $\mathbf{det(...) = 0}$ for k (complex quantity, in general)

Linear stability analysis

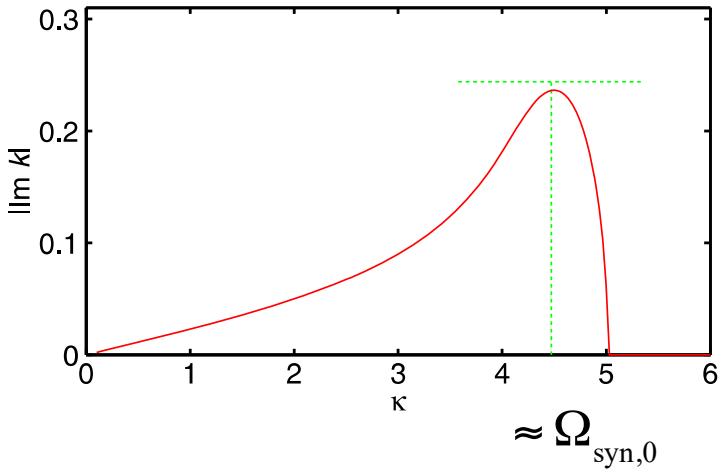

- Im $k > 0$: growth
- Maximum growth rate corresponds to $\Omega_{syn,0}$, the electron synchrotron frequency
- For untapered FEL, the sideband growth rate remains a constant along z
- For tapered FEL, we may expect z-dependent growth rate

Numerical simulations

- Use LCLS-like beam and undulator parameters
- Taper profile assumed constant-Θ_R, starting location not optimized
- 1-D simulation, only focus on sideband dynamics
- Particle simulation results need postprocessing to extract sideband information

TABLE I. Numerical parameters for the beam, undulator and radiation fields for the hard x-ray FELs.

Name	Value	Unit
Electron beam energy	10.064	GeV
RMS relative energy spread	10^{-4}	
Peak current	4	kA
Normalized emittances (x, y)	0.3,0.3	μm-rad
Average beta function (x, y)	5,5	m
Undulator parameter K_0 (peak)	3.5	
Undulator period	3	cm
Input seed power	1	MW
Resonance wavelength	2.755/4.5	Å/keV
First saturation power	~80	GW
First saturation length	~13	m

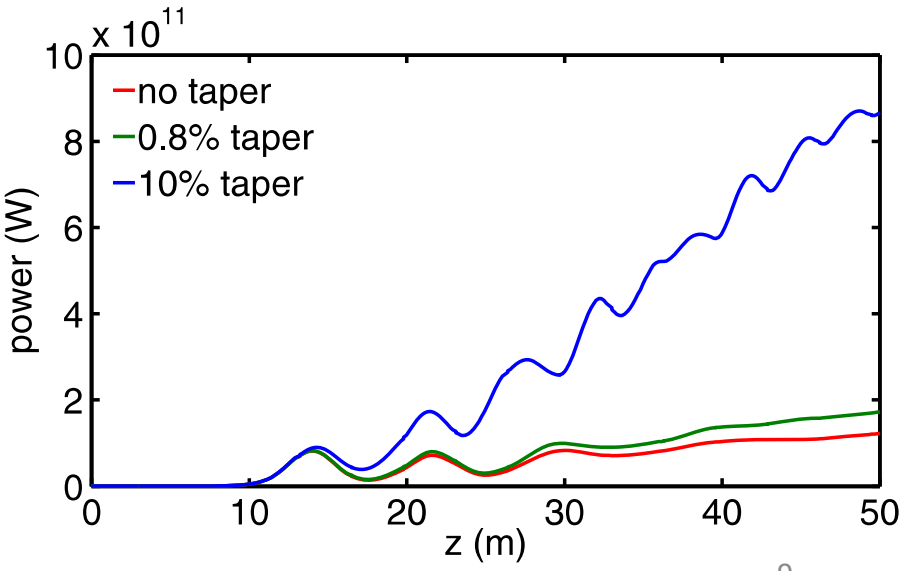

Data postprocessing

- The sideband spectrum can be fluctuating
  - each longitudinal slice responds slight differently
  - within a slice, electron finite energy spread may result in spread of synchrotron/sideband frequency ➔ finite sideband bandwidth

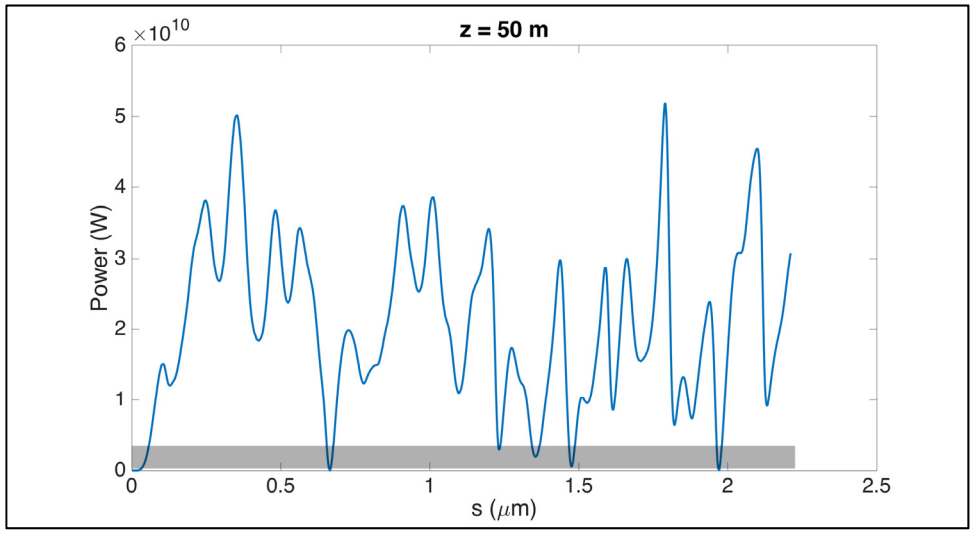

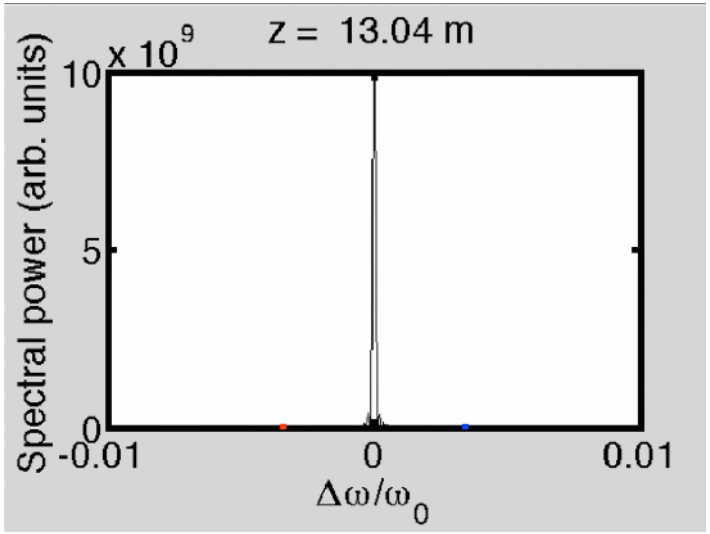

Data postprocessing

- Locate the sideband frequency by $\omega_s^{\pm} \approx \omega_0 \pm 2c\gamma_R^2 \Omega_{\mathrm{syn},0}$ (lower and upper)

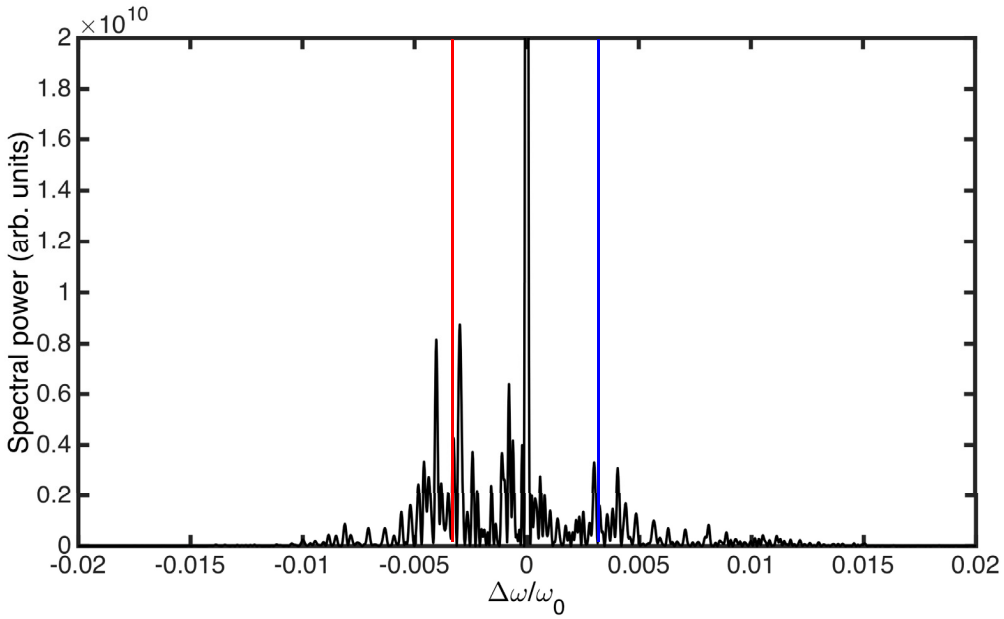

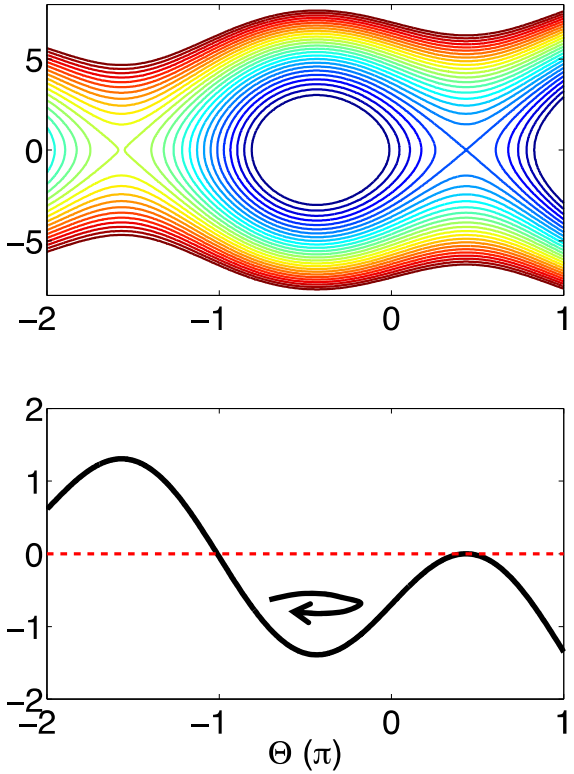

Data postprocessing

- Locate the sideband frequency by $\omega_s^{\pm} \approx \omega_0 \pm 2c\gamma_R^2\Omega_{\mathrm{syn},0}$ (lower and upper)
- Estimate the spread of sideband (due to finite electron energy spread)

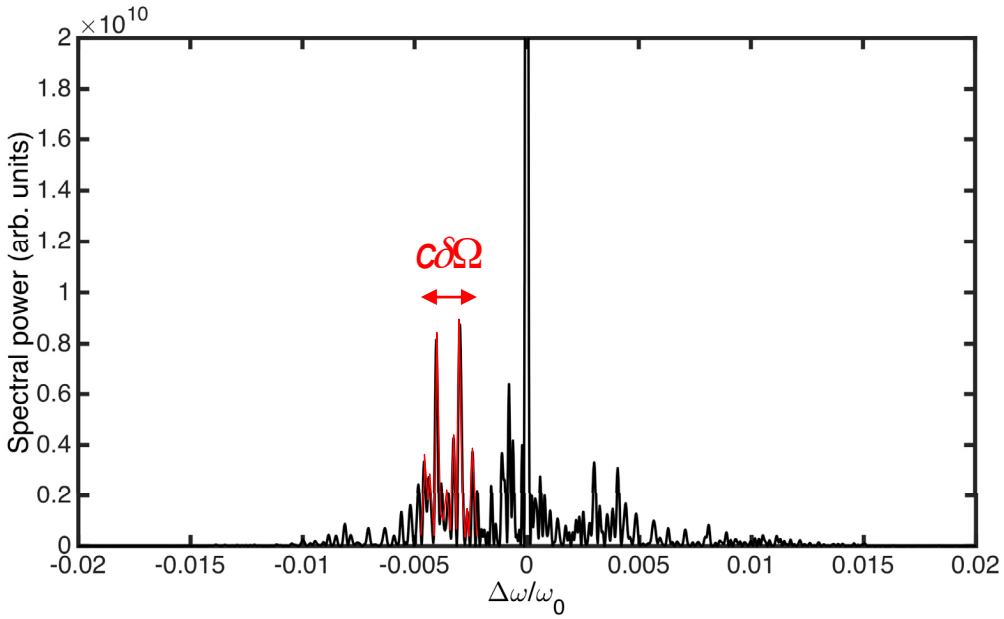

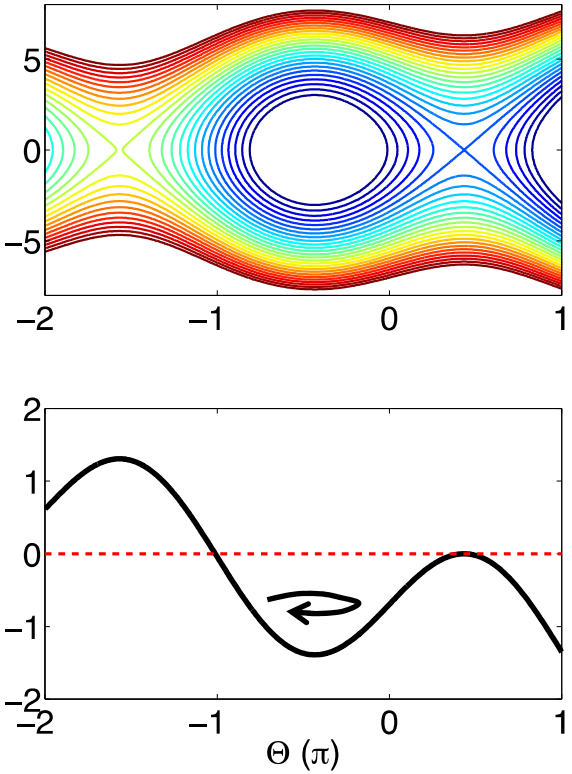

Data postprocessing

- Locate the sideband frequency by $\omega_s^{\pm} \approx \omega_0 \pm 2c\gamma_R^2\Omega_{\mathrm{syn},0}$ (lower and upper)
- Estimate the spread of sideband (due to finite electron energy spread)
- Take average on the finite sideband bandwidth
- Identify the sideband field

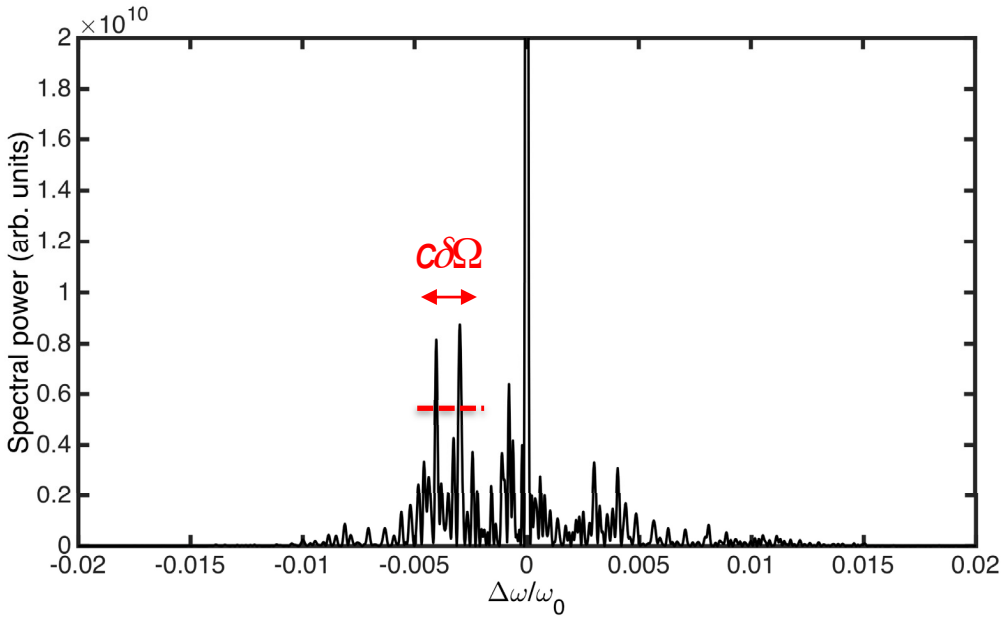

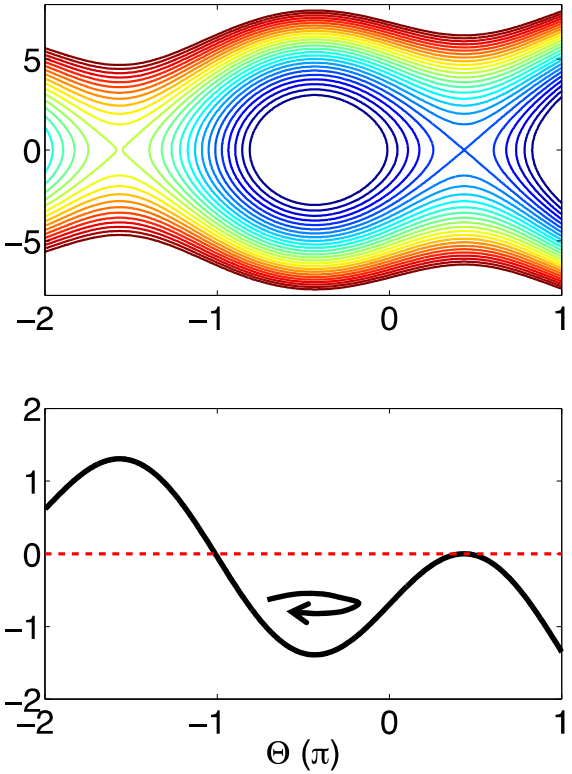

$$G(\hat{z}) \equiv \left| \frac{\mathcal{E}_s(\hat{z})}{\mathcal{E}_s(\hat{z}_b)} \right| = e^{\Lambda(\hat{z})}$$

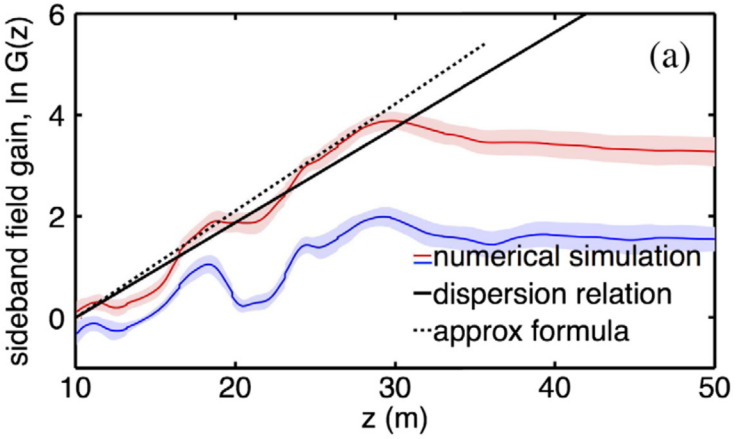

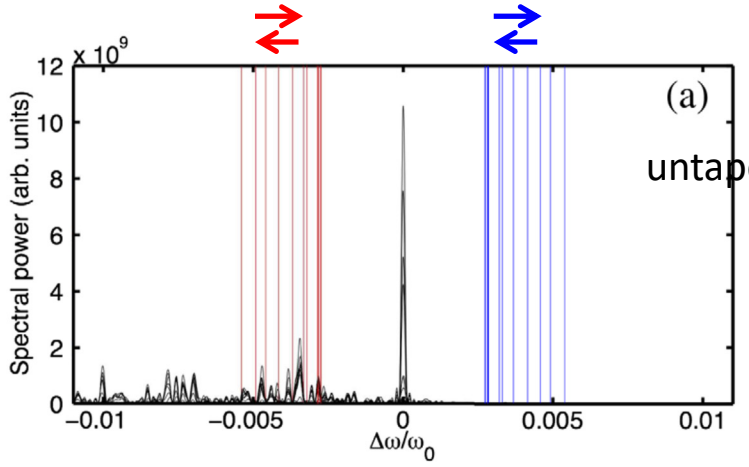

untapered

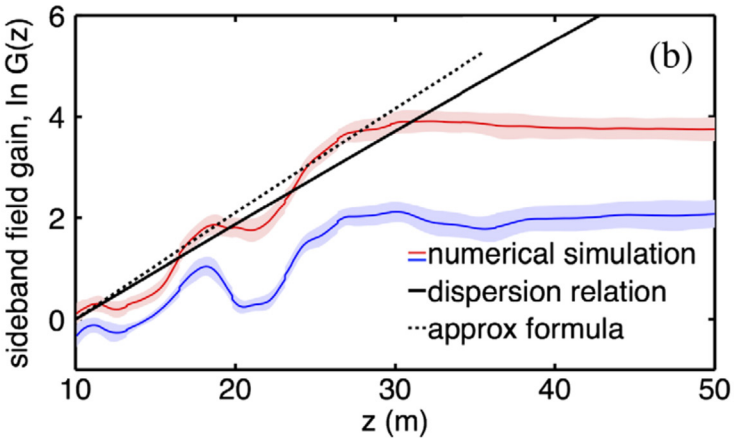

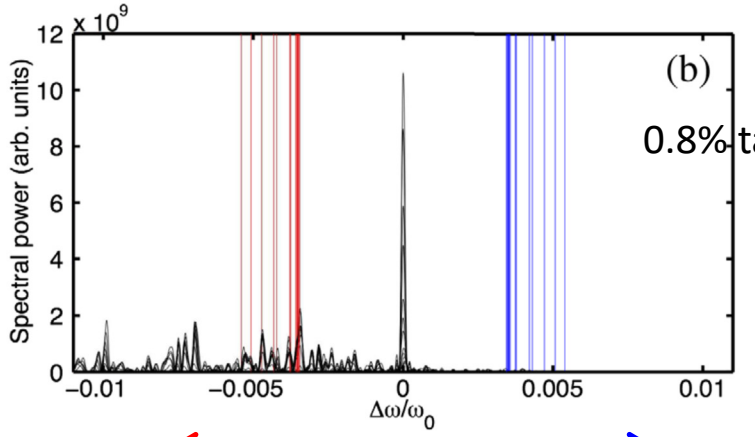

0.8% taper

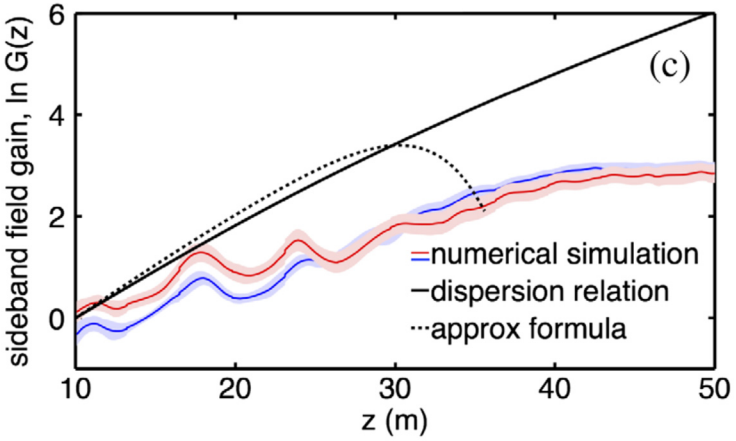

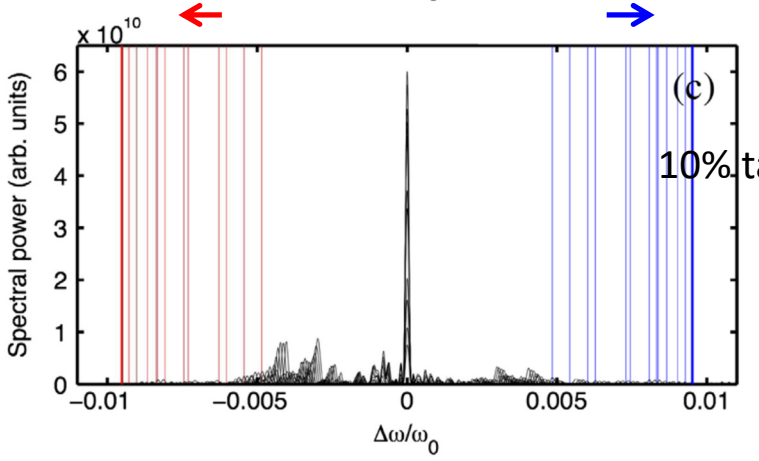

10% taper

Numerical simulations

- Another way to quantify the sideband contribution is to define the integrated sideband-to-main-signal power ratio

$$R(\Delta) \equiv \frac{\text{spectral power outside } 2\rho}{\text{spectral power within } 2\rho} = \frac{\square + \square}{\square}$$

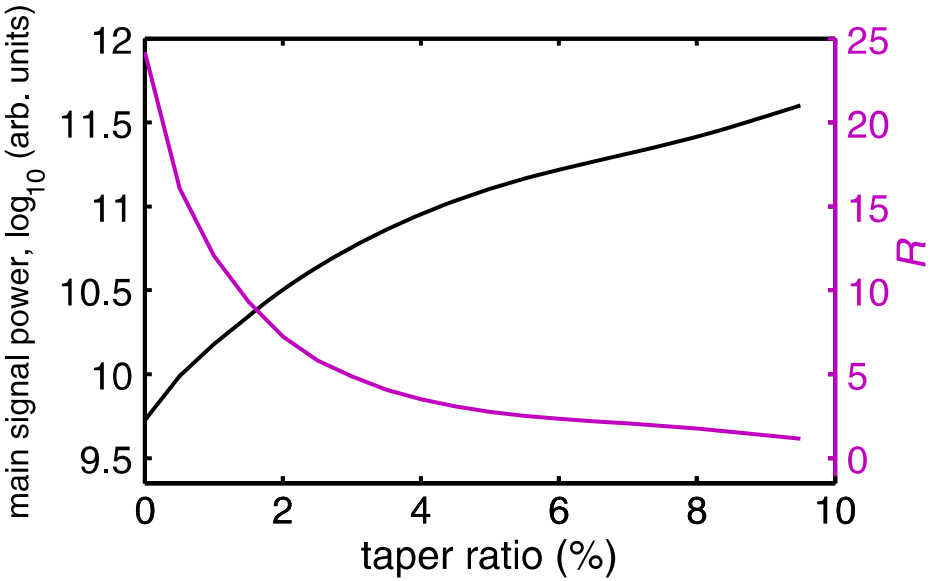

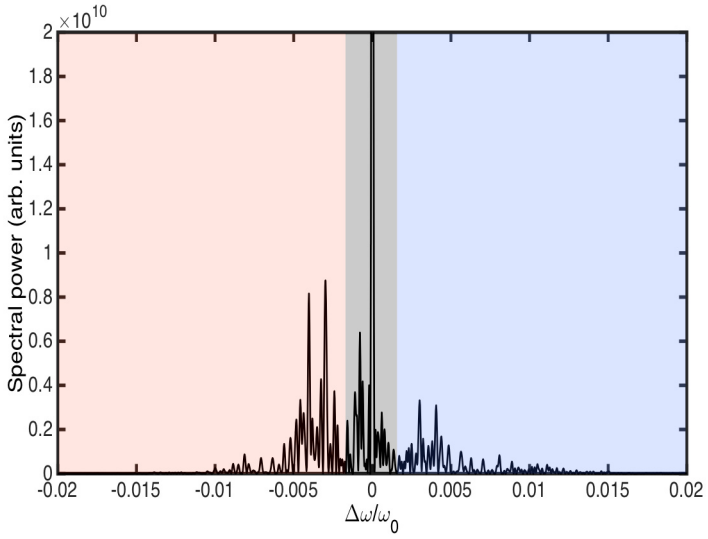

averaged over 50 independent runs for each taper ratio Δ

Part I: Summary and Discussion

- In tapered case, the synchrotron sideband frequency tends to **sweep away** from the main signal
- From the macroparticle analysis, we find that **strong** undulator tapering can help **mitigate** sideband instability in the post-saturation regime
- Effects of undulator tapering on the sideband growth *simply* go into z-dependence of the relevant quantities, e.g., taper profile f_B, main-signal resonance energy change f_R, $\left|\mathcal{E}_0(\hat{z})\right|$ and $\Omega_{syn,0}(\hat{z})$
- Comparison of macroparticle model with the 1-D numerical simulation gives **qualitative agreement**
- Other remaining issues for the theoretical model
  - effect of finite-depth electrons in the potential well (we have noticed this when postprocessing the particle simulation results) or the effect of finite energy spread not included
  - the asymmetric sideband growth, transient sideband evolution, effect of various phase space distributions on sideband growth, and second saturation need to be further investigated

Part II

TRANSVERSE DIFFRACTION IN POST-SATURATION TAPERED FEL

Ref: C.-Y. Tsai *et al*., PRAB **21**, 060702 (2018)

Transverse diffraction, refractive & gain guiding

- In the **linear** regime the compensation effect (balance) between the natural tendency of radiation diffraction and the presence of electron beam lead to the refractive & gain guiding
- Kroll, Morton and Rosenbluth (1981), Moore & Scharlemann *et al*. (1985)

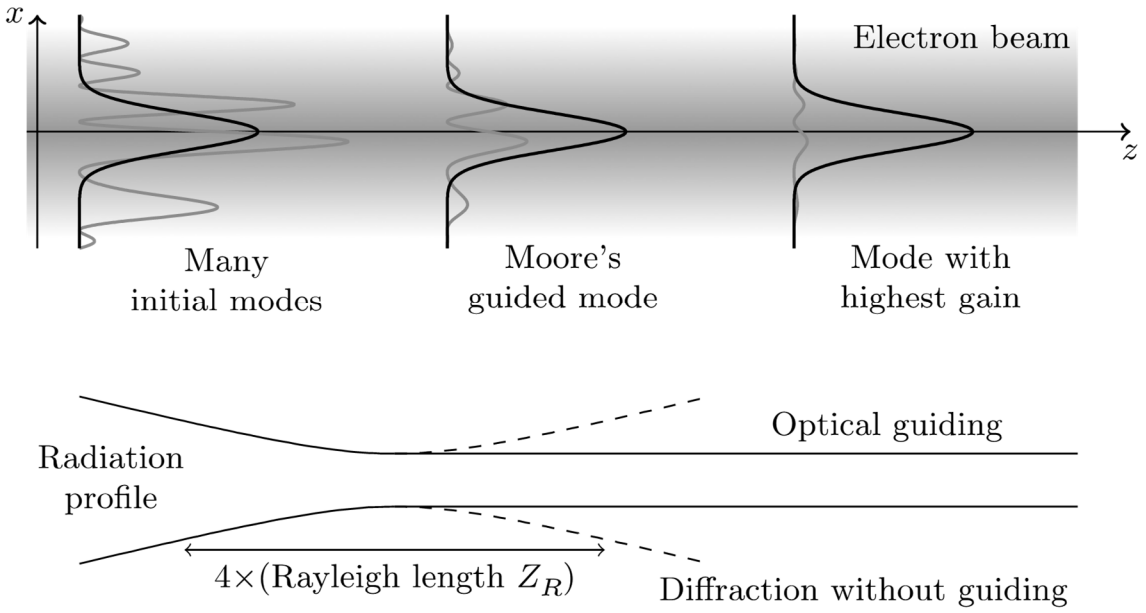

Kim, Huang, and Lindberg, Synchrotron radiation and free electron lasers, Cambridge University Press (2017)

Transverse diffraction in post-saturation regime

- In the **post-saturation** regime, the gain guiding effect becomes reduced by less rapidly growing radiation and gradually increasing radiation beam size
- In the semi-analytical analysis, we rely on the constants of motion (or system invariants)

Analysis in post-saturation regime

- Two constants of motion
  - energy conservation $|\mathcal{E}(\hat{z})|^2 + \langle \eta \rangle = C_1$
  - z-independent Hamiltonian

    Gluckstern *et al*., PRE (1993), Huang and Kim, NIMA (2002) for untapered case

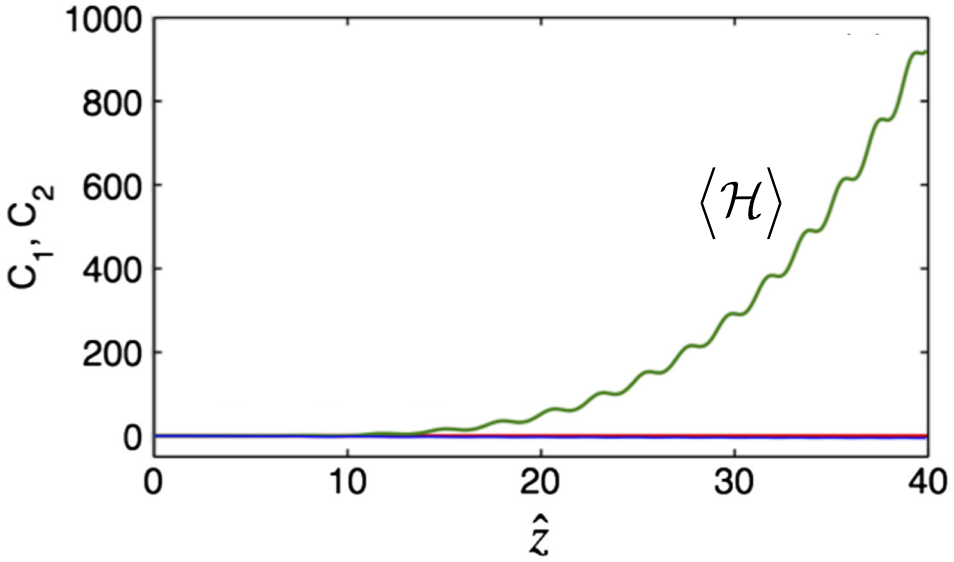

Analysis in post-saturation regime

- Two constants of motion
  - energy conservation $|\mathcal{E}(\hat{z})|^2 + \langle \eta \rangle = C_1$
  - ~~z-independent Hamiltonian~~ phase space action variable $\langle \mathcal{H}(\hat{z}) \rangle / \Omega_{\mathrm{syn}}(\hat{z}) = C_2$

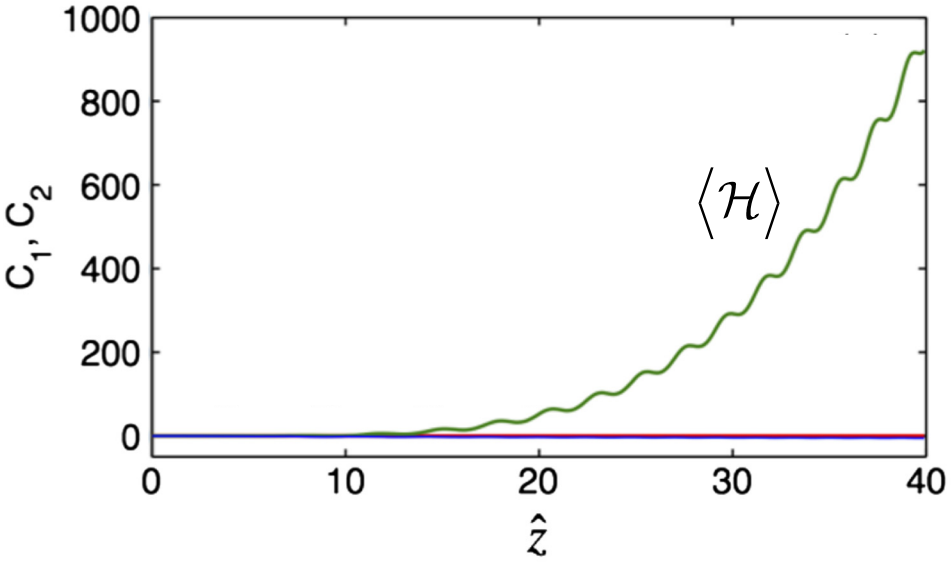

Analysis in post-saturation regime

- Two constants of motion
  - energy conservation $|\mathcal{E}(\hat{z})|^2 + \langle\eta\rangle = C_1$
  - ~~z-independent Hamiltonian~~ phase space action variable $\langle\mathcal{H}(\hat{z})\rangle/\Omega_{\rm syn}(\hat{z}) = C_2$
- Parameterize the solution of the radiation field as

field dynamics

$$\mathcal{E} = (P + iQ)e^{i\Phi} \qquad \Phi \approx \kappa_0 + \kappa_1(\hat{z} - \hat{z}_0) + \frac{\kappa_2}{2}(\hat{z} - \hat{z}_0)^2$$

growing part

oscillating part

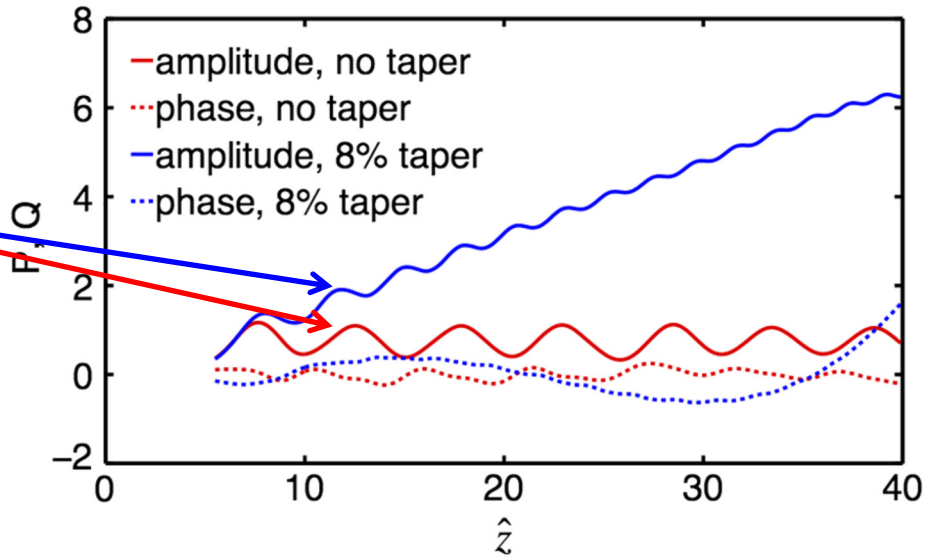

Analysis in post-saturation regime

- Two constants of motion
  - energy conservation $|\mathcal{E}(\hat{z})|^2 + \langle\eta\rangle = C_1$
  - ~~z-independent Hamiltonian~~ phase space action variable $\langle\mathcal{H}(\hat{z})\rangle/\Omega_{\rm syn}(\hat{z}) = C_2$
- Parameterize the solution of the radiation field as

field dynamics

$$\mathcal{E} = (P + iQ)e^{i\Phi} \qquad \Phi \approx \kappa_0 + \kappa_1(\hat{z} - \hat{z}_0) + \frac{\kappa_2}{2}(\hat{z} - \hat{z}_0)^2$$

growing part

oscillating part

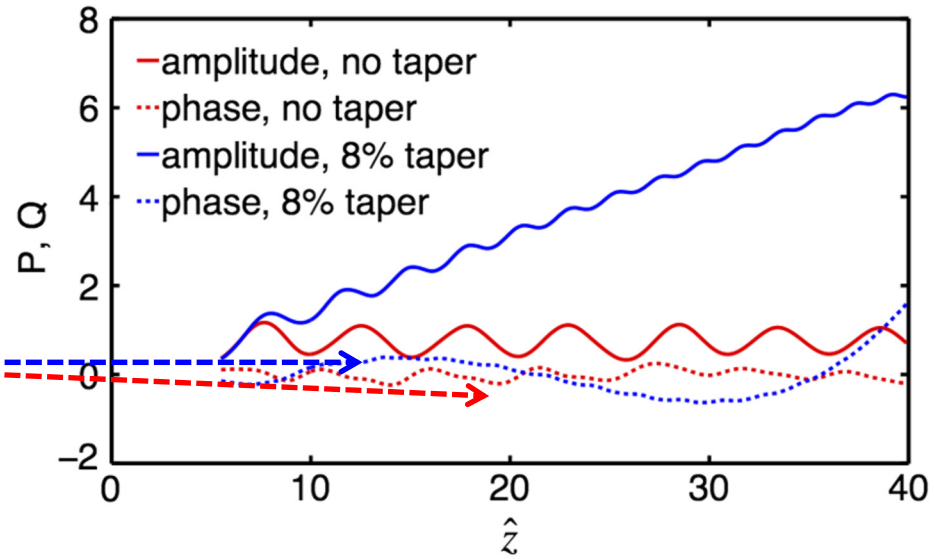

Analysis in post-saturation regime

- Two constants of motion
  - energy conservation $|\mathcal{E}(\hat{z})|^2 + \langle\eta\rangle = C_1$
  - ~~z-independent Hamiltonian~~ phase space action variable $\langle\mathcal{H}(\hat{z})\rangle/\Omega_{\rm syn}(\hat{z}) = C_2$

field dynamics

- Parameterize the solution of the radiation field as

$$\mathcal{E} = (P + iQ)e^{i\Phi} \qquad \Phi \approx \kappa_0 + \kappa_1(\hat{z} - \hat{z}_0) + \frac{\kappa_2}{2}(\hat{z} - \hat{z}_0)^2$$

electron dynamics

- Assume the electron phase space distribution takes the form

$$f_{\rm BZM} = \mathcal{N} e^{-\alpha\tilde{I}(\beta,\beta';\hat{z})}$$

α : particle energy spread in the potential well
β : displaced electron phase from bottom well
$\tilde{I}$: C_2 expressed in the new coordinate

- Field equation including the transverse diffraction

$$\frac{\partial\mathcal{E}}{\partial\hat{z}} - i\nabla_\perp^2\mathcal{E} = \frac{f_B(\hat{z})}{f_R(\hat{z})}U(\hat{r})\langle e^{-i\theta}\rangle$$

Transverse diffraction in post-saturation regime

- FEL power efficiency

$$f_R\kappa_1 - \eta_R = \frac{\int \hat{r}d\hat{r}P^2(\hat{r};\hat{z})}{\int \hat{r}d\hat{r}U(\hat{r})}$$

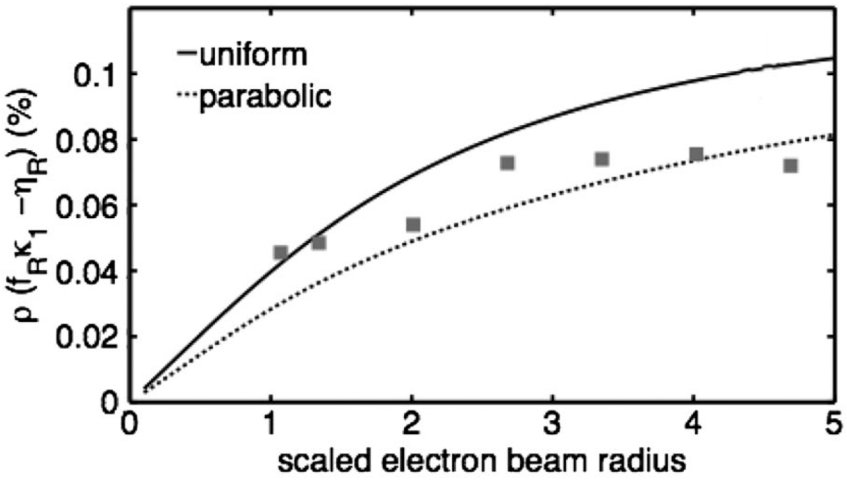

$$\hat{r} = \sqrt{4\rho k_u k_R} r$$

ρ ≈ 1.5 × 10^{-3}, based on LCLS-like parameters

Transverse diffraction in post-saturation regime

- FEL power efficiency

$$f_R\kappa_1 - \eta_R = \frac{\int \hat{r}d\hat{r}P^2(\hat{r};\hat{z})}{\int \hat{r}d\hat{r}U(\hat{r})}$$

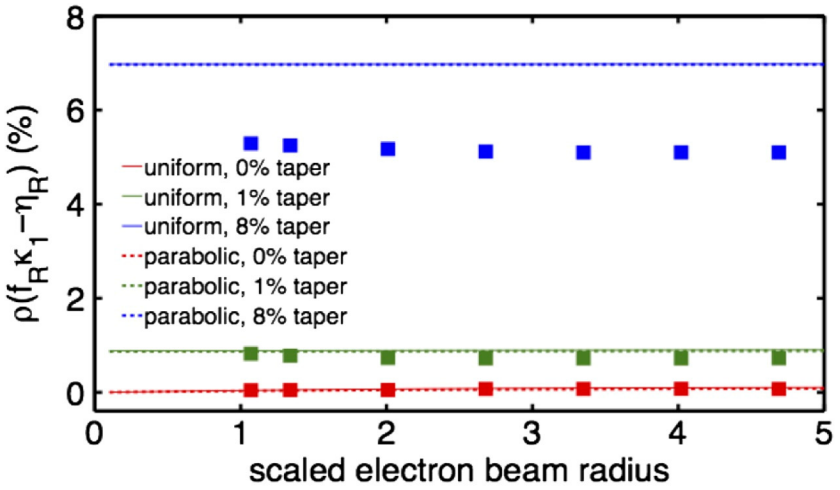

$$\hat{r} = \sqrt{4\rho k_u k_R}\, r$$

Almost **independence** on the transverse beam size
(Note: the analysis assumed finite beam size but still zero beam emittance, i.e., no betatron motion)

Transverse diffraction in post-saturation regime

- FEL power efficiency

$$f_R\kappa_1 - \eta_R = \frac{\int \hat{r}d\hat{r}P^2(\hat{r};\hat{z})}{\int \hat{r}d\hat{r}U(\hat{r})}$$

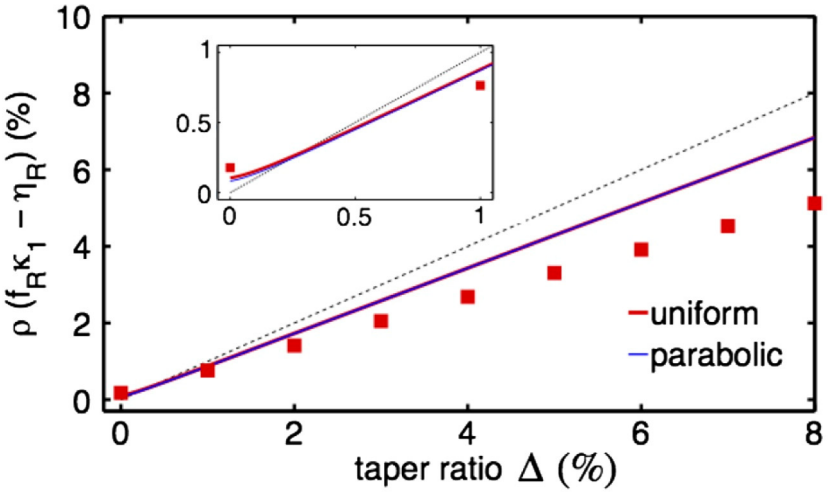

Power efficiency ≤ total taper ratio Δ (≠0)

Transverse diffraction in post-saturation regime

- Transverse radiation field profile

untapered

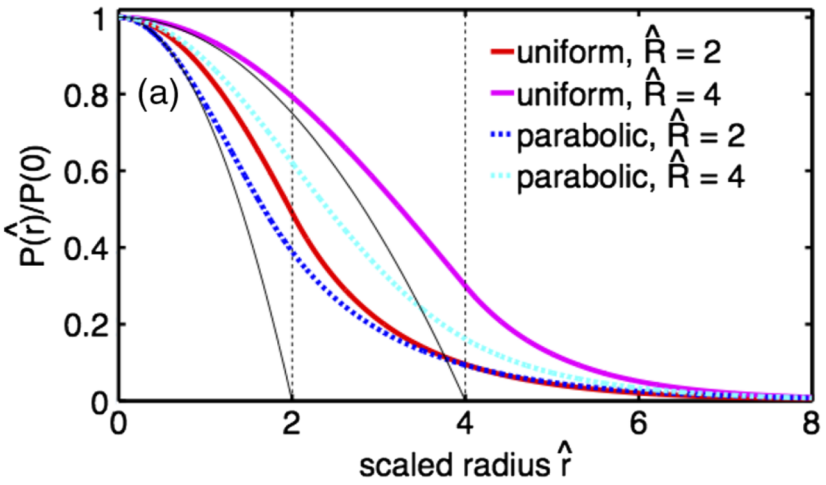

More of the enhanced radiation field is contributed **from outside** of the transverse electron beam **than inside**

8% taper

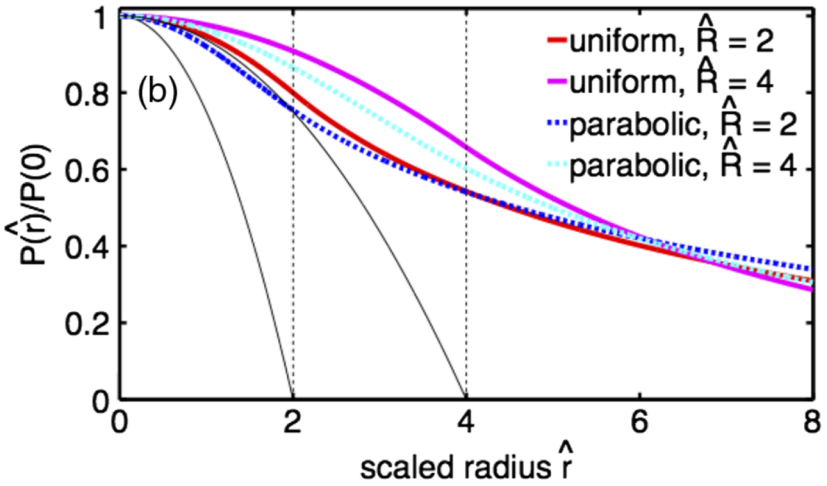

Transverse diffraction in post-saturation regime

- GENESIS simulation

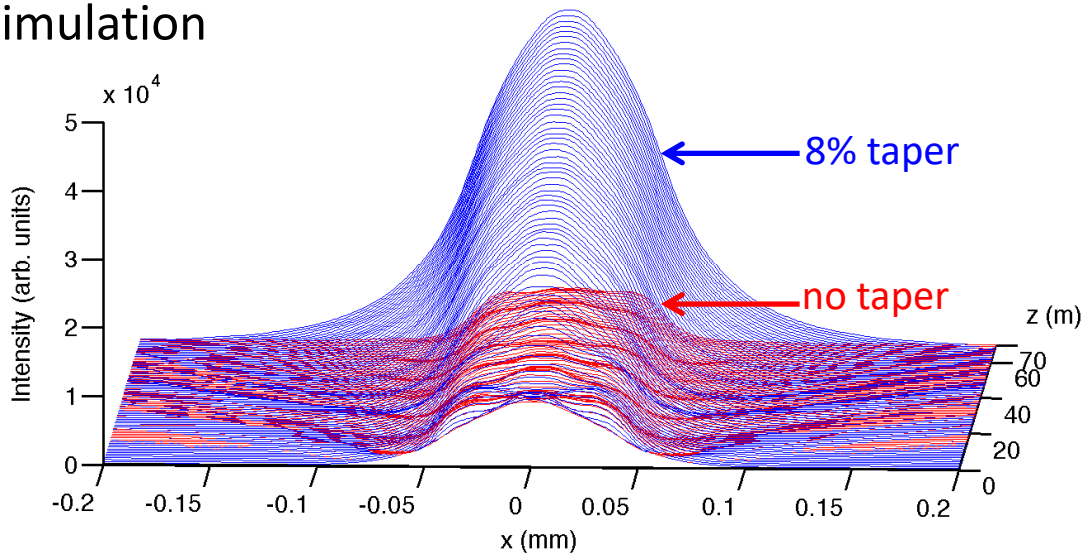

$$\frac{P_{\text{inside ebeam}}}{P_{\text{outside ebeam}}}$$

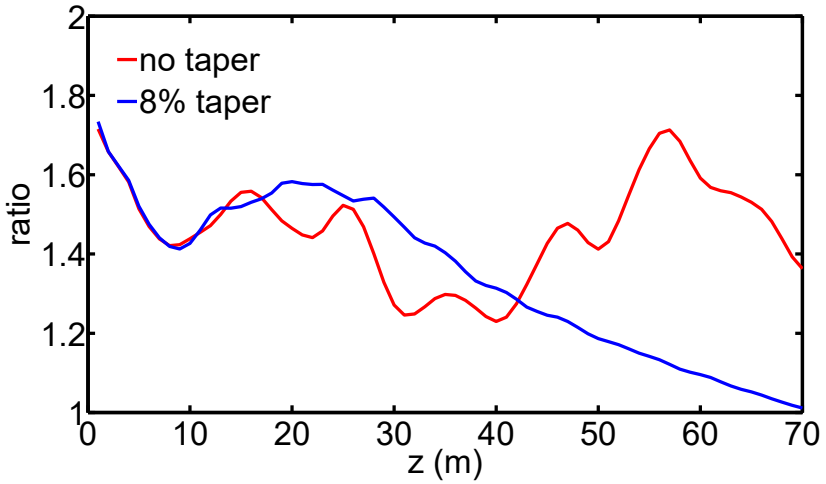

Part II: Summary and Discussion

- Although FEL dynamics in the post-saturation regime becomes more involved than the linear regime, we may analyze it by taking advantage of the integrals of motion
- Tapered power efficiency is **almost independent** on the transverse beam size (for the case of weak or absent transverse focusing)
- Tapered power efficiency can be close to (smaller than) the total taper ratio, if the taper design is optimized
- In the deep saturation regime, **more** field intensity is contributed from **outside** of the transverse electron beam **than** that from **inside**
- Other remaining issues for the theoretical model
  - Further extension of the semi-analytical formulation to include transverse electron beam emittance should provide a useful tool for FEL design consideration of post-saturation undulator line
  - combine with sideband instability analysis

Part III

AREA-PRESERVING TAPER SCHEMES FOR HIGH-EFFICIENCY FEL

Ref: C.-Y. Tsai *et al*., NIMA **913**, 107-119 (2019)

1-D analysis: action-angle transform

- To better capture the phase space bucket characteristics $(\theta,\eta)\leftrightarrow(\varphi,J)$

$$\mathcal{H}(\theta,\eta;\hat{z})=\frac{(\eta-\eta_R)^2}{2f_R}-i\frac{f_B}{f_R}\left(\mathcal{E}e^{i\theta}-\mathcal{E}^*e^{-i\theta}\right)=\frac{(\delta\eta)^2}{2f_R}+2\frac{f_B(\hat{z})}{f_R(\hat{z})}|\mathcal{E}|\left[\sin\Theta_R+\sin\Theta-(\Theta+\Theta_R)\cos\Theta_R\right]$$

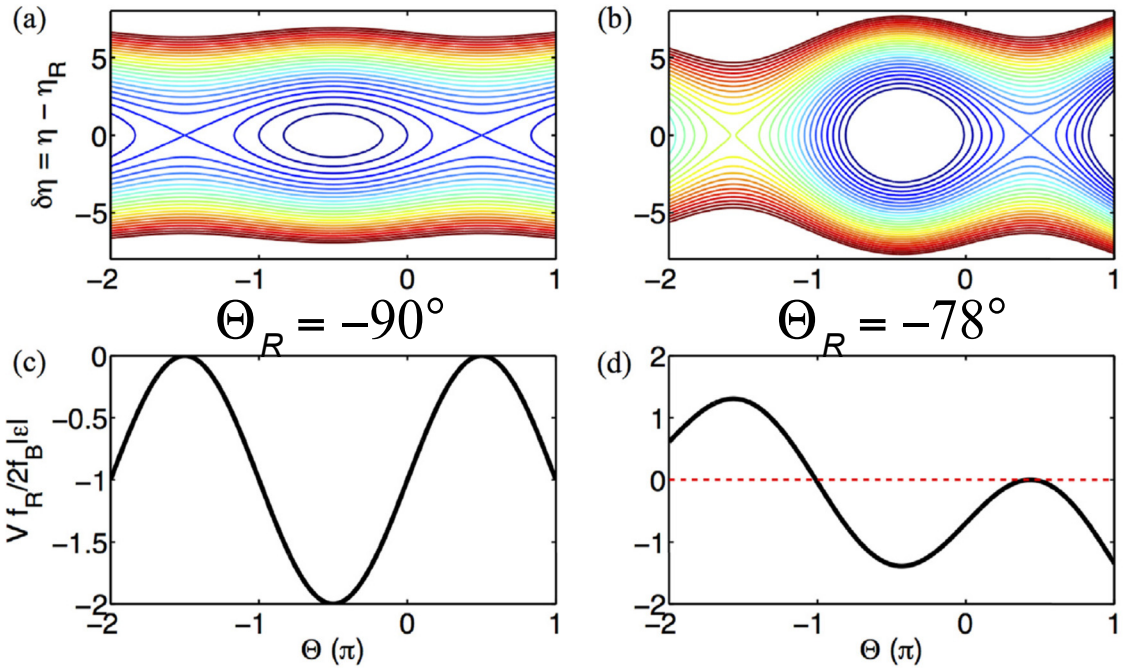

Energy extraction in post-saturation tapered FEL

- Involves two main physical mechanisms:
- 1) **bucket deceleration**: phase space bucket moving *downward* to give energy to the radiation field
- 2) **particle detrapping**: some particles executing large amplitude will detrap

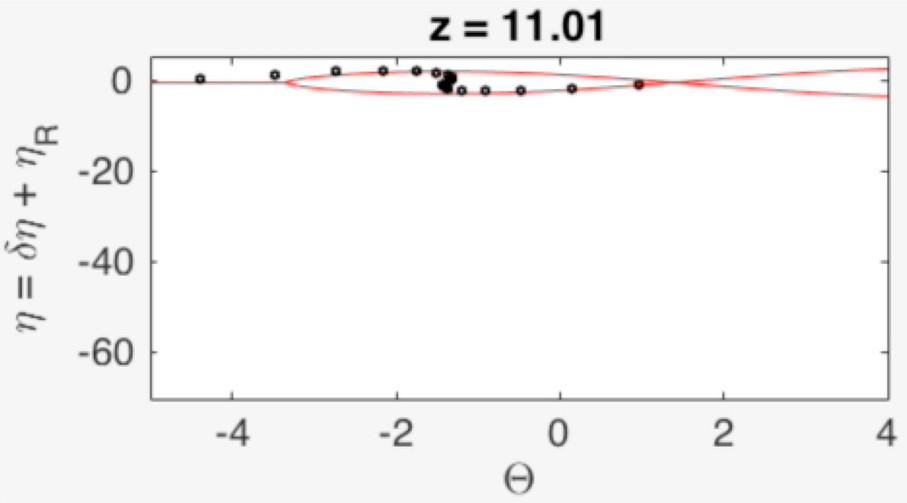

Energy extraction in post-saturation tapered FEL

- Involves two main physical mechanisms:
- 1) **bucket deceleration**: phase space bucket moving *downward* to give energy to the radiation field
- 2) **particle detrapping**: some particles executing large amplitude will detrap

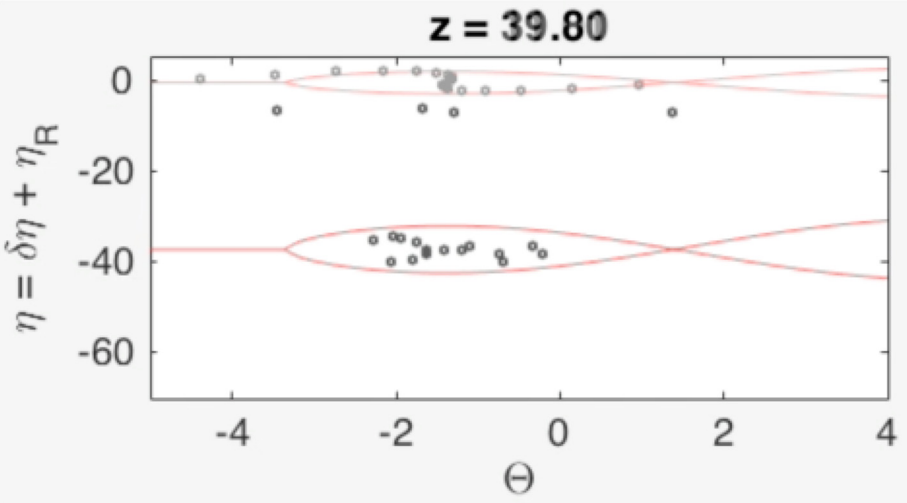

Energy extraction in post-saturation tapered FEL

- Involves two main physical mechanisms:
- 1) **bucket deceleration**: phase space bucket moving *downward* to give energy to the radiation field
- 2) **particle detrapping**: some particles executing large amplitude will detrap
- The desire of undulator tapering for efficiency enhancement is to **precipitate** the bucket deceleration process, and, in the meanwhile, to **keep as many as possible** the electrons in the phase space bucket

Constant-Θ_R taper scheme

- Kroll, Morton, and Rosenbluth, IEEE QE **17**, 1436-1468 (1981)
- Undulator taper profile follows constant-Θ_R along z
- The optimum efficiency can be close to 14% at Θ_R = -50° (coasting beam)

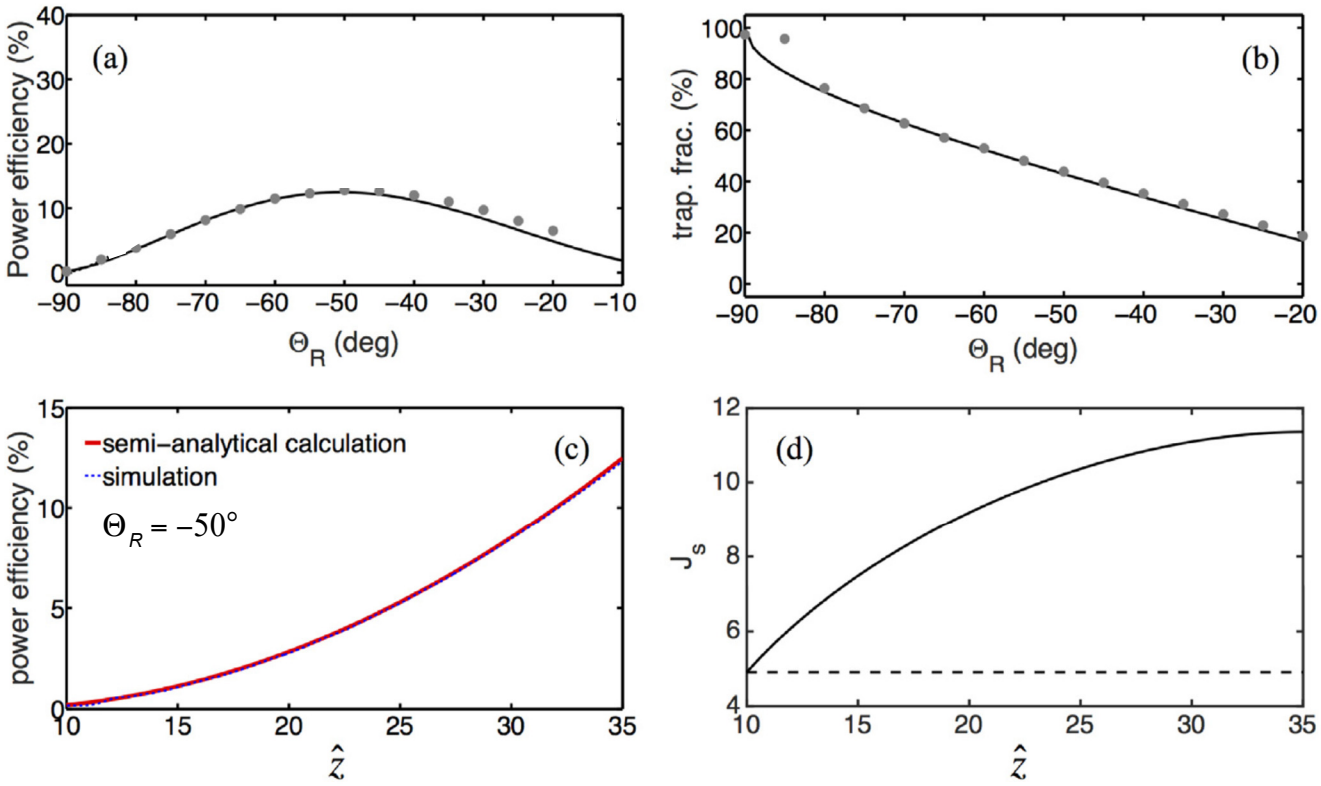

Constant-Θ_R taper with prebunched beam

- C. Emma *et al.*, PRAB **20**, 110701 (2017)
- Undulator taper profile follows constant-Θ_R along *z*, and the beam at the initial saturation is prebunched
- The optimum efficiency can be close to 40% at Θ_R = -35°

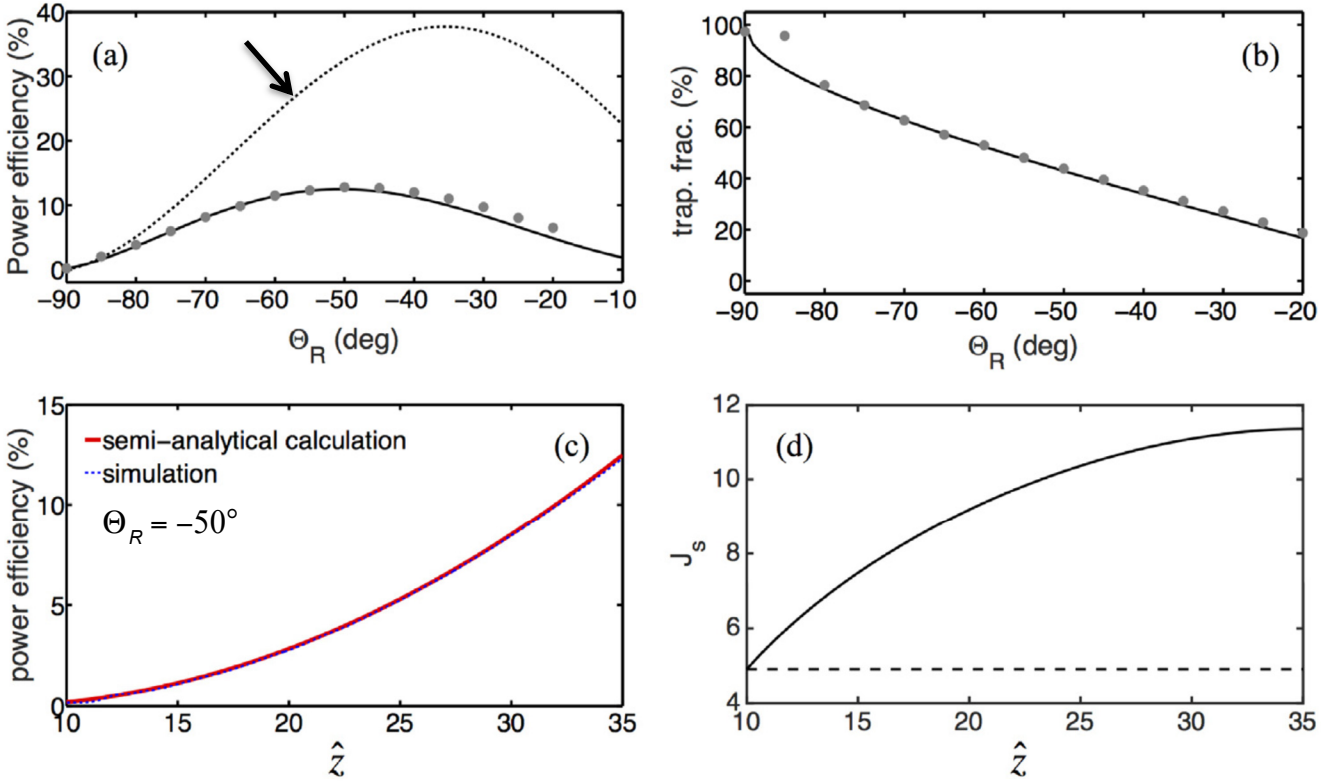

Linear-Θ_R taper scheme

- Mak, Curbis, and Werin, PRAB **18**, 040702 (2015) $\Theta_R(\hat{z}) = g_1(\hat{z} - \hat{z}_b) - \pi/2$
- Linear-Θ_R scheme takes care of initial particle detrapping, but the (unnecessary) bucket area remains increasing in the deep saturation regime
- The optimum efficiency ranges from 10% and 35%, depending on the undulator length

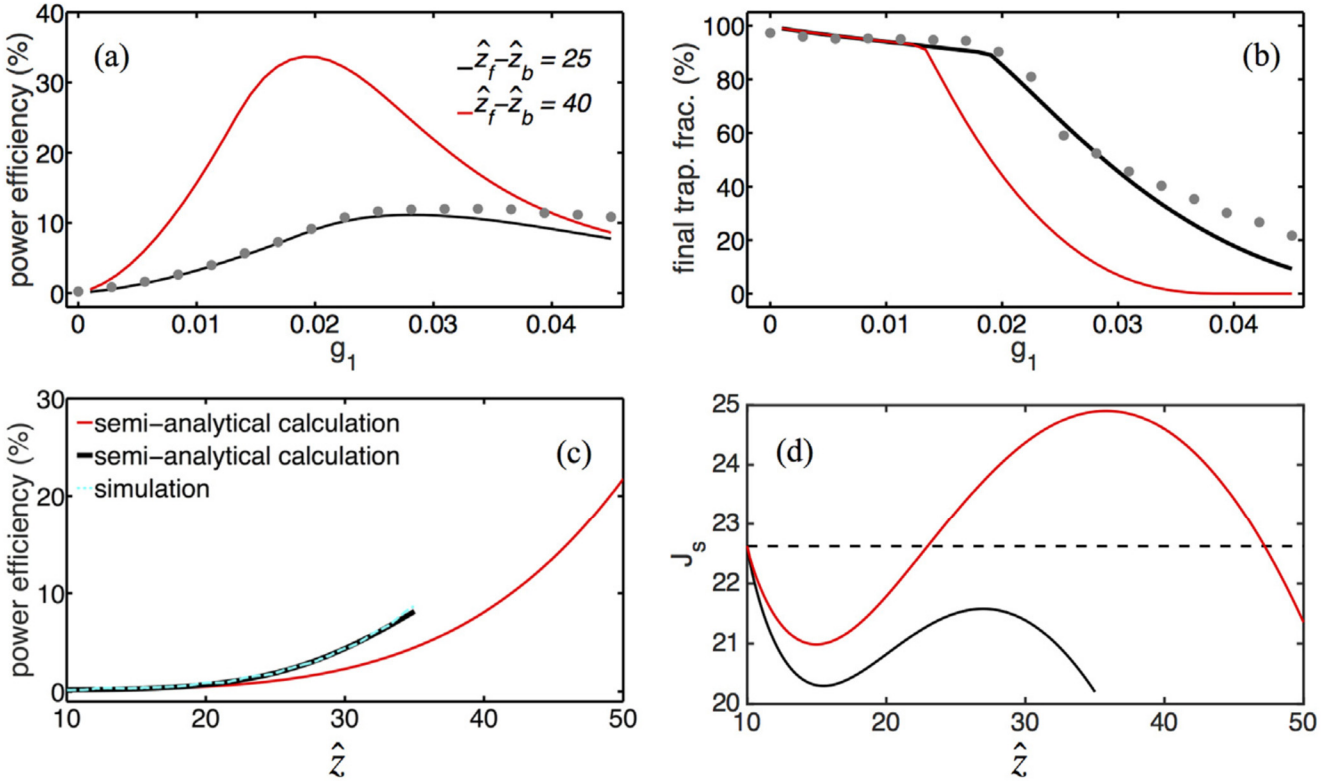

Area-preserving taper scheme

- Bucket deceleration and particle detrapping are both taken care
- The phase space area remains constant, as a result of balance between the growing radiation field and the effect of increasing Θ_R
- The optimum efficiency can be close to 20% (coasting beam)

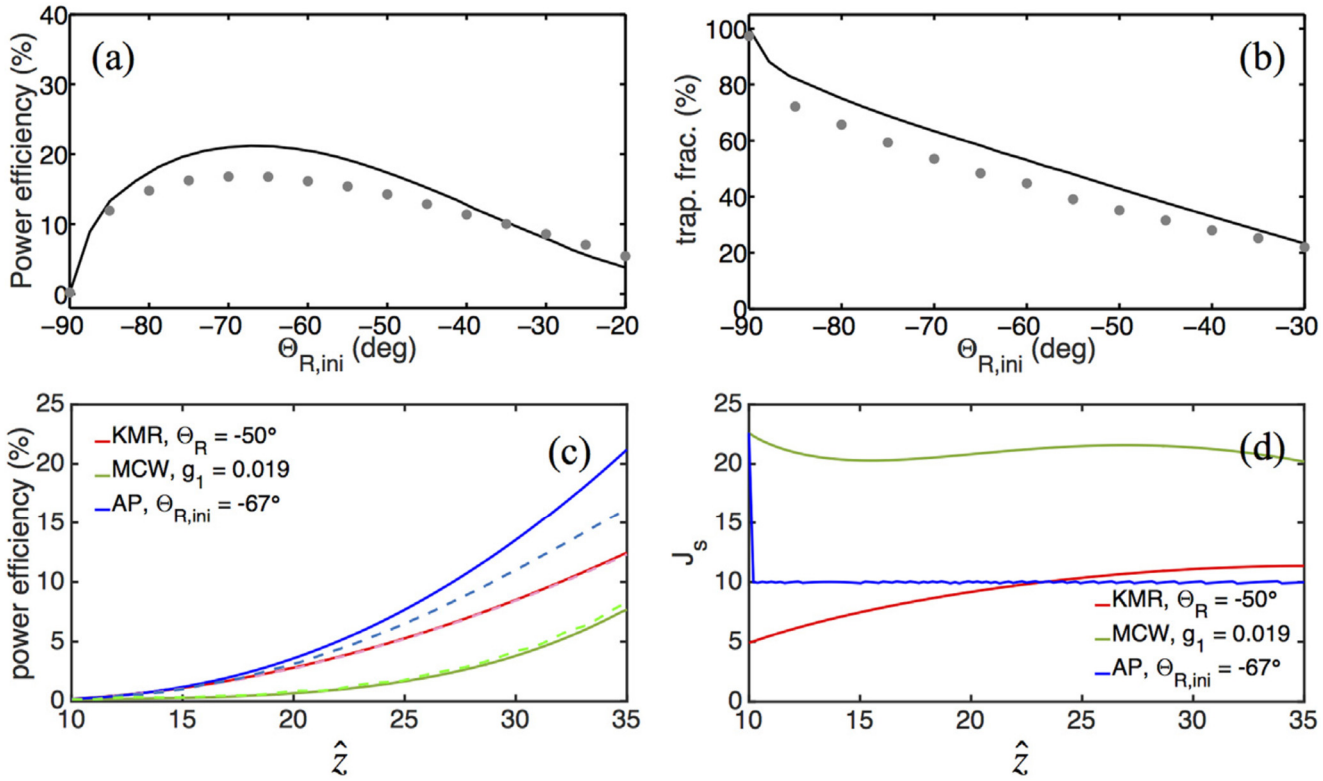

Area-preserving taper scheme

- Bucket deceleration and particle detrapping are both taken care
- The phase space area remains constant, as a result of balance between the growing radiation field and the effect of increasing Θ_R
- The optimum efficiency can be close to 50% (prebunched beam)

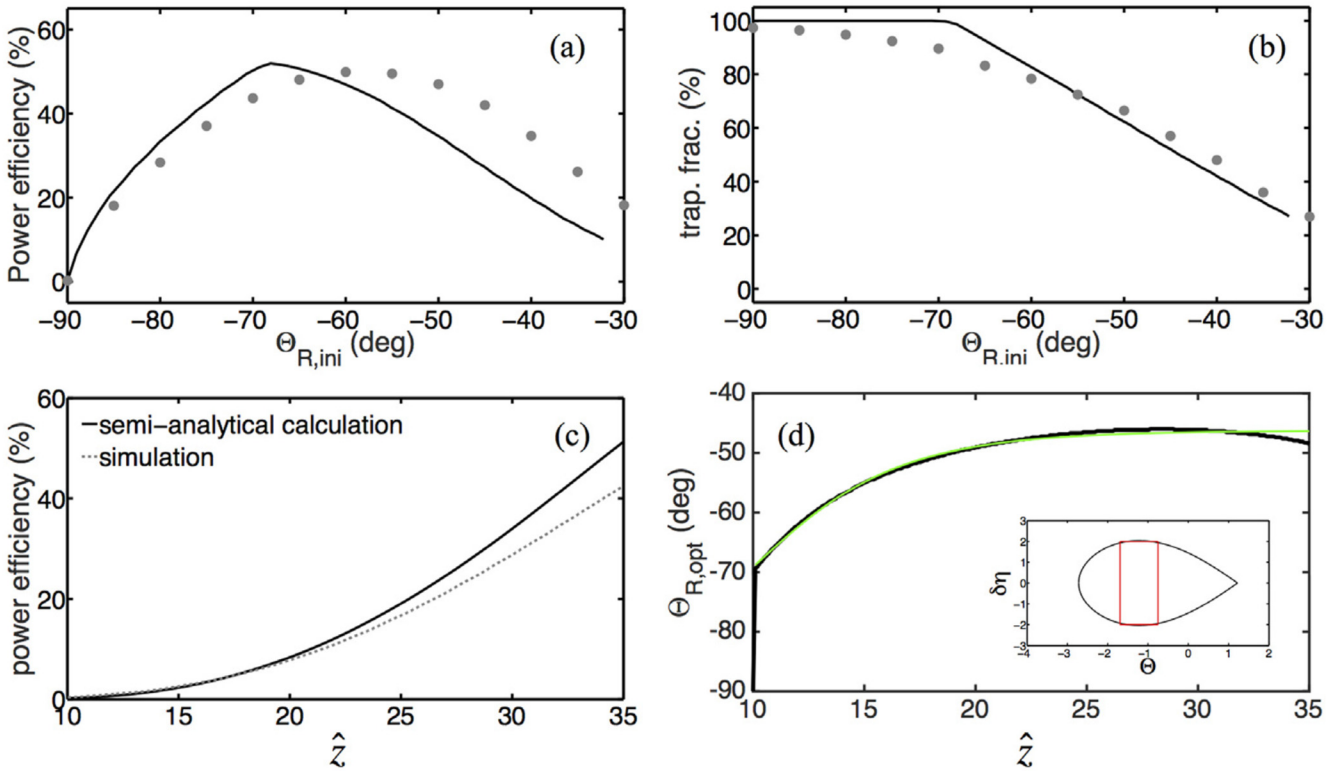

semi-analytical expression of taper profile

Numerical simulation

- Use perave [C. Emma, https://github.com/cemma1/FEL_code_PBPL]

Name	Value	Unit
Electron beam energy	4.5	GeV
RMS relative energy spread	3.3×10^{-4}	
Peak current	4	kA
Undulator period	2	cm
Undulator parameter (rms)	3	
Resonant wavelength	12.4/1	Å/keV
Pierce FEL parameter	2×10^{-3}	

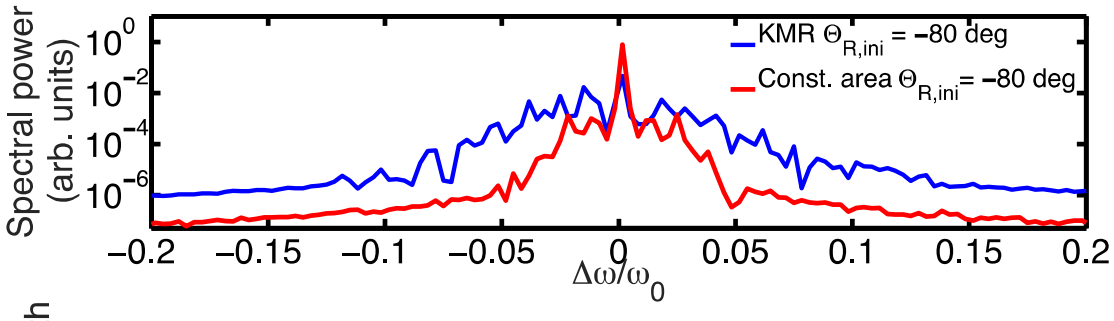

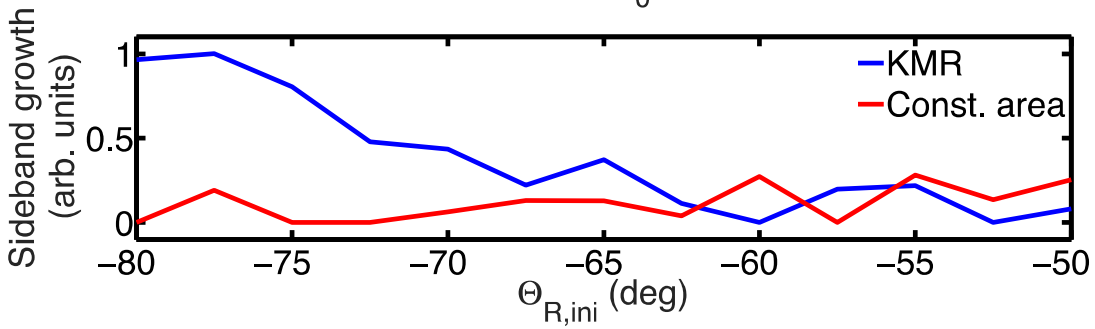

Numerical simulation

- Use perave [C. Emma, https://github.com/cemma1/FEL_code_PBPL]

Name	Value	Unit
Electron beam energy	4.5	GeV
RMS relative energy spread	3.3×10^{-4}	
Peak current		kA
Undulator period	2	cm
Undulator parameter (rms)	3	
Resonant wavelength	12.4/1	Å/keV
Pierce FEL parameter	2×10^{-3}	

Effective suppression of FEL sideband instability over wide range of Θ_R!

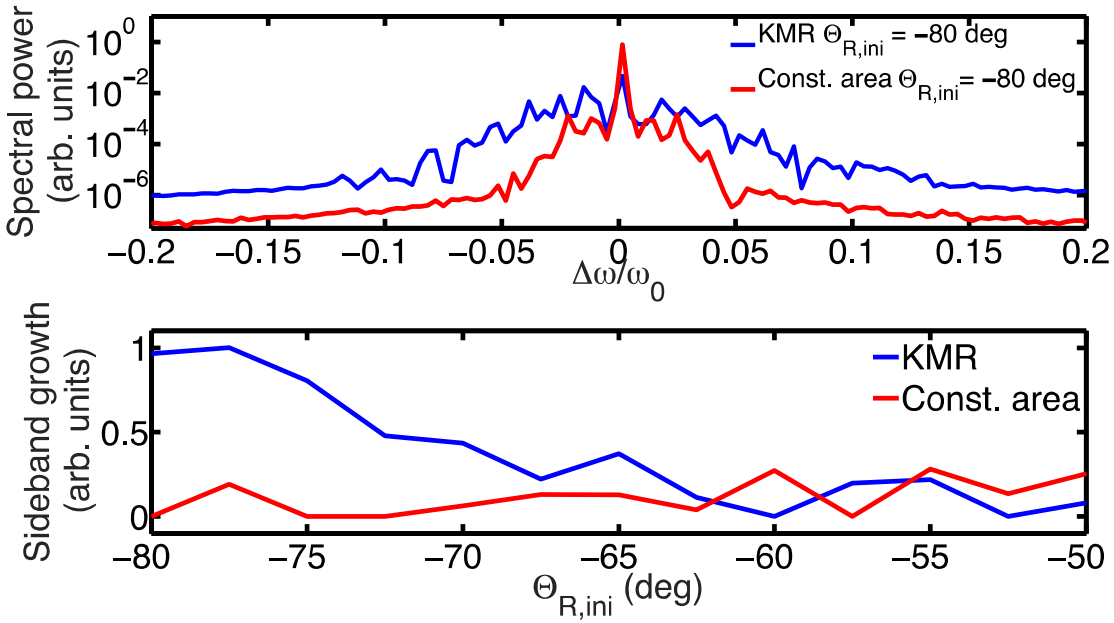

Part III: Summary and Discussion

- By including two trade-off mechanisms in post-saturation tapered FEL (**bucket deceleration** and **particle detrapping**), in the semi-analytical analysis, the area-preserving taper scheme takes **both** effects into consideration for evaluation of FEL output power performance
- 1-D time-dependent simulations indicate that such a taper scheme can also **effectively suppress FEL sideband instability**
- Other remaining issues for the theoretical model
  - include transverse diffraction (and finite-emittance electron beam) into the analysis, which will lead to additional particle detrapping
  - analyze the sideband instability in such a Θ_R-varying case

- *Work in progress*: combined analyses of the aforementioned three issues

Acknowledgements

- Thank **Siegfried Schreiber** and **Gianluca Geloni** for the invitation
- Thanks to my postdoc supervisor, co-authors, colleagues for their kind support, insights, and stimulating discussions
  - **Juhao Wu** (SLAC), **Claudio Emma** (SLAC), **Moohyun Yoon** (POSTECH), **Alex Chao, Yunhai Cai** (SLAC)
  - **Guanqun Zhou** (IHEP), **Xiaofan Wang** (SINAP), **Chuan Yang** (ShanghaiTech)
- This work was supported by U.S. Department of Energy (DOE) under Contract No. DE-AC02-76SF00515 and the U.S. DOE Office of Science Early Career Research Program Grant No. FWP-2013- SLAC-100164, and by the Fundamental Research Funds for the Central Universities under Project No. 5003131049

References

- In this presentation I must have missed the references. We refer the interested reader to the papers below (and references therein)

❑ **Part I**

– Cheng-Ying Tsai, Juhao Wu, Chuan Yang, Moohyun Yoon, and Guanqun Zhou, Sideband instability analysis based on a one-dimensional high-gain free-electron laser model, PRAB **20**, 120702 (2017)

❑ **Part II**

– Cheng-Ying Tsai, Juhao Wu, Chuan Yang, Moohyun Yoon, and Guanqun Zhou, Single-pass high-gain tapered free-electron laser with transverse diffraction in the postsaturation regime, PRAB **21**, 060702 (2018)

❑ **Part III**

– Cheng-Ying Tsai, Claudio Emma, Juhao Wu, Moohyun Yoon, Xiaofan Wang, Chuan Yang, and Guanqun Zhou, Area-preserving scheme for efficiency enhancement in single-pass tapered free electron lasers, NIMA **913**, 107-119 (2019)

Thank you for your attention